

## Study of the $(p, t)$ Reaction on the Even Gadolinium Nuclei

Donald G. Fleming

*Department of Chemistry, University of British Columbia, Vancouver 8, British Columbia, Canada*

Christian Günther

*Institut für Strahlen- und Kernphysik, Universität Bonn, Bonn, Germany*

Gudrun Hagemann and Bent Herskind

*The Niels Bohr Institute, University of Copenhagen, Copenhagen, Denmark*

Per O. Tjømm

*Institute of Physics, University of Oslo, Oslo, Norway*

(Received 2 April 1973)

The  $(p, t)$  reaction has been studied at 18 MeV on all the stable even-even Gd targets. A strong population of both  $0^+$  and  $2^+$  excited states has been found; the  $0^+$  ( $\beta$  vibrations) in the deformed nuclei are all  $\approx 15\%$  of the ground-state cross sections. The shape transition at  $N=88$  is observed in the  $^{154}\text{Gd}(p, t)^{152}\text{Gd}$  reaction: Two excited  $0^+$  states are strongly populated. In the deformed Gd nuclei, a distinction between  $K=0$  and  $K=2$   $2^+$  states can be made on the basis of the shapes of their angular distributions. The spectrum observed in the  $^{152}\text{Gd}(p, t)^{150}\text{Gd}$  reaction is characteristic of that expected on spherical nuclei, with a relatively strong population of an excited  $0^+$  state. Distorted-wave Born-approximation calculations are highly successful in fitting the  $0^+$  transitions but, generally, not the  $2^+$  and higher spin states.

NUCLEAR REACTIONS, NUCLEAR STRUCTURE  $^{160-152}\text{Gd}(p, t)^{158-150}\text{Gd}$ ,  $E=18$  MeV; measured  $\sigma(\theta)$ ; resolution 12 keV. Enriched targets. DWBA analysis.

### I. INTRODUCTION

In recent years, the  $(t, p)$  and  $(p, t)$  reactions have provided important new information on the structure of deformed nuclei at  $150 \lesssim A \lesssim 186$ . To date, such data have been reported in the even isotopes of Ce, Nd, Sm, Gd, Dy, Er, Yb, and W,<sup>1-10</sup> as well as some work in the odd- $A$  isotopes of Tb and Pr.<sup>11</sup>

The isotopes of Ce and Nd are predominantly spherical nuclei and the measured  $(p, t)$  and  $(t, p)$  spectra on the even targets reflect this fact. The g.s. transition in this mass region does not generally collect all the  $0^+$  strength and the observed yield to excited  $0^+$  states has been interpreted in terms of pair vibrations. The lowest-lying (vibrational)  $2^+$  state is also relatively strongly populated.

The nuclei from Nd to Gd cross the onset of nuclear deformation at  $N=88$  and the observed two-neutron transfer data on these nuclei correspondingly reflect marked changes in nuclear structure; this is manifest by a sudden strong population of an excited  $0^+$  state. Indeed, much of the evidence

for "shape transitions" in this mass region has been derived from studies of  $(t, p)^2$  and  $(p, t)^{3-6}$  reactions on the appropriate isotopes. The term "coexistence model" has been coined to describe  $0^+$  states of both spherical and deformed shape in the same nucleus and the two-neutron transfer results have prompted theoretical studies to describe their structure.<sup>12</sup>

In the heavier deformed nuclei, the collective structure is also reflected in the two-neutron transfer data—the  $0^+$ ,  $2^+$ ,  $4^+$  members of the g.s. rotational band, as well as  $\beta$  and  $\gamma$  vibrational  $2^+$  states are all populated.<sup>3-10</sup> The ground states of the deformed nuclei are generally superconducting so that, just as in a spherical nucleus, the g.s.  $(p, t)$  transition would be expected to collect essentially all of the  $0^+$  strength. The data in the rare-earth nuclei, on the other hand, show a relatively strong and stable population of excited  $0^+$  states.<sup>4-7, 9</sup> Similar data have been reported in the tungsten<sup>10</sup> and actinide<sup>13</sup> nuclei. Much theoretical interest is currently focusing on these states and they will be referred to again in the discussion to follow.

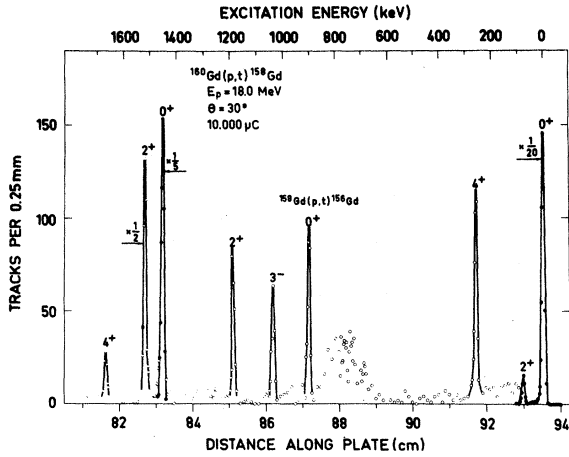


FIG. 1. Energy spectrum at  $30^\circ$  for the  $^{160}\text{Gd}(p,t)^{158}\text{Gd}$  reaction at 18 MeV. The energy resolution is typically 12 keV.

With its emphasis on a collective form factor [unlike the  $(p, d)$  reaction], a systematic study and theoretical interpretation of the  $(p, t)$  and/or  $(t, p)$  reaction in deformed nuclei will be important in furthering our understanding of nuclear structure in this region. Accordingly, we would like to report herein on the  $(p, t)$  data obtained on all the stable even-even Gd targets. The final nuclei reached in this two-neutron pickup reaction span the region from spherical ( $A=150$ ) to stably deformed ( $A=158$ ) and include the "quasirotational" nucleus  $^{152}\text{Gd}$ ; the reaction  $^{154}\text{Gd}(p, t)^{152}\text{Gd}$  crosses the region of nuclear deformation at neutron number  $N=88$ . It is important that nuclear models for both the reaction dynamics and the intrinsic structure be able to reproduce the correct overall picture for these nuclei rather than in just a limited region. The present  $(p, t)$  data should

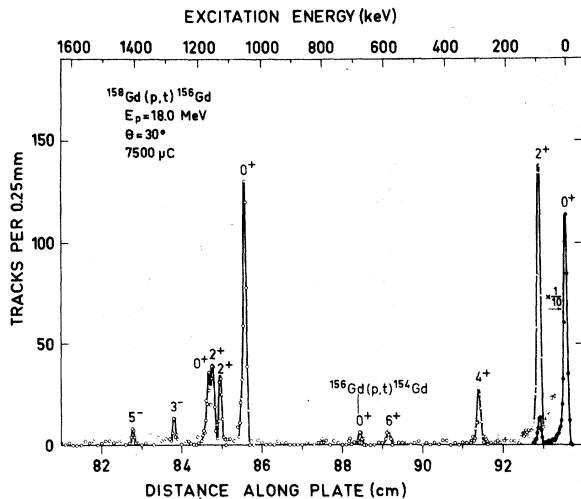


FIG. 2. Energy spectrum at  $30^\circ$  for the  $^{158}\text{Gd}(p,t)^{156}\text{Gd}$  reaction at 18 MeV.

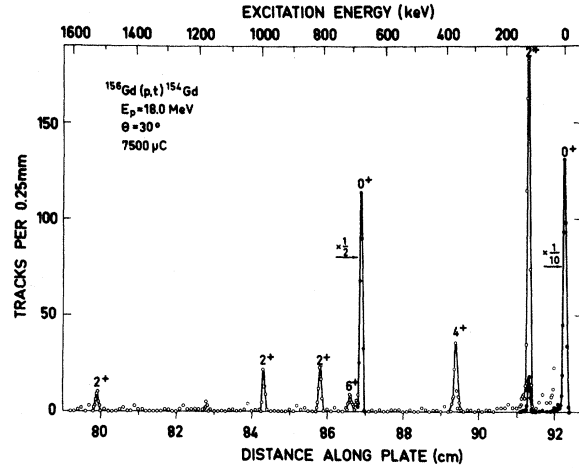


FIG. 3. Energy spectrum at  $30^\circ$  for the  $^{156}\text{Gd}(p,t)^{154}\text{Gd}$  reaction at 18 MeV.

provide an adequate test of such models. A preliminary report of these data, concerned mainly with the  $0^+$  states observed, can be found in Ref. 5. After our work was completed, similar experiments were reported by Elze, Boyno, and Hui-zenga.<sup>6</sup> Their results will be compared with ours below.

## II. EXPERIMENTAL RESULTS

These experiments were carried out using the 18-MeV proton beam of the FN tandem accelerator at the Niels Bohr Institute. Outgoing tritons were detected in photographic plates placed in the focal plane of the magnetic spectograph. The  $^{160}\text{Gd}$ ,  $^{158}\text{Gd}$ , and  $^{156}\text{Gd}$  targets were prepared by evaporation of the corresponding oxide (enriched to  $\approx 95\%$ ) onto carbon backings. For the long ex-

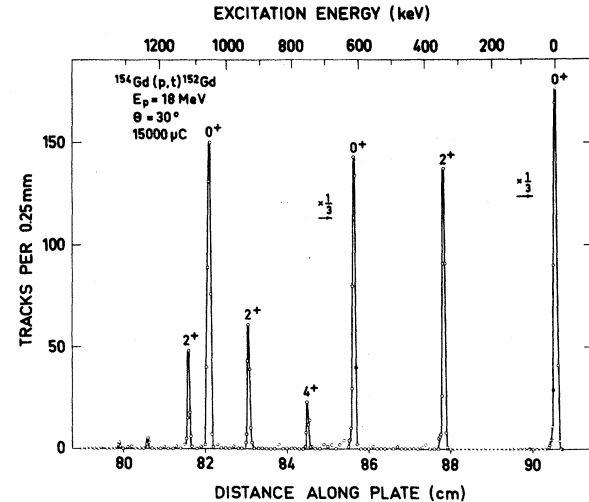


FIG. 4. Energy spectrum at  $30^\circ$  for the  $^{154}\text{Gd}(p,t)^{152}\text{Gd}$  reaction at 18 MeV.

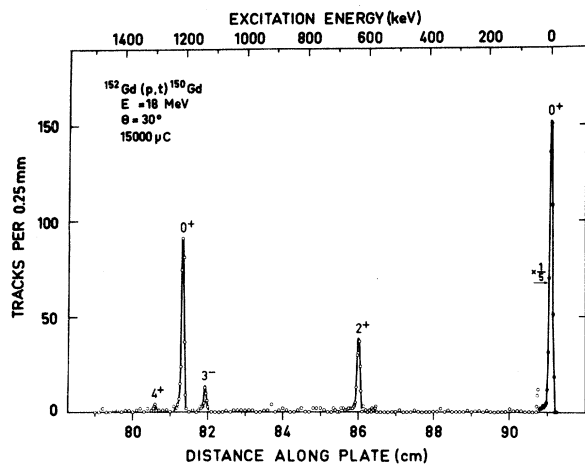


FIG. 5. Energy spectrum at  $30^\circ$  for the  $^{152}\text{Gd}(p,t)^{150}\text{Gd}$  reaction at 18 MeV.

posures ( $15\,000 \mu\text{C}$ ) on  $^{154}\text{Gd}$  and  $^{152}\text{Gd}$ , the targets used were prepared by implantation of the separated isotope into a carbon foil. Thin aluminum strips were placed over the plates to absorb low-energy deuterons and  $\alpha$  particles; there was no contamination from  $(p,d)$  or  $(p,t)$  reactions in the carbon backing because of low  $Q$  values. Representative spectra (at  $30^\circ$  lab) are shown in Figs. 1–5. The range of excitation studied in each case was 0–2 MeV. No measurable strength was observed beyond 2 MeV. The energy resolution was typically 12 keV.

For the reaction  $^{160}\text{Gd}(p,t)^{158}\text{Gd}$  ( $160 \rightarrow 158$ ), complete angular distributions were taken in  $5^\circ$  steps in the range  $5\text{--}80^\circ$ ; for the reaction ( $154 \rightarrow 152$ ) the range covered was  $7.5\text{--}70^\circ$  in steps of  $7.5^\circ$ . For the latter reaction the complete g.s. angular distribution was also measured with an evaporated target, (i.e., in addition to the isotope-separated target) enriched to 45% in  $^{154}\text{Gd}$ . Less complete data were obtained on the other targets; the ( $158 \rightarrow 156$ ) reaction was measured at  $15, 30, 45,$  and  $60^\circ$ , while these same angles plus  $22.5$  and  $37.5^\circ$  were recorded for the ( $156 \rightarrow 154$ ) reaction. For the ( $152 \rightarrow 150$ ) reaction, data were only obtained on the isotope-separated target at angles of  $15, 20, 30,$  and  $45^\circ$ ; the cross-section normalization for these runs is less certain than for the other targets. Nevertheless, the similarity in shapes of the angular distributions for a given state allowed the extraction of a summed yield in all cases; this is given in Table I for the range  $5\text{--}70^\circ$ .

The observed angular distributions for 18-MeV  $(p,t)$  reactions on the Gd nuclei are shown in Figs. 6–11. The absolute cross sections were determined from a measurement of the proton elastic scattering at forward angles (where it is essential-

ly pure Rutherford) and are believed to be accurate to  $\pm 20\%$ . The relevant data are given in Table I, for target nuclei  $A=160$  to  $A=152$ . In addition, several checks were performed on the relative cross sections for the g.s. transitions on all the Gd targets at an angle of  $30^\circ$  (lab), including two exposures ( $10\,000 \mu\text{C}$ ) on a specially prepared evaporated target which was enriched in  $^{152}\text{Cd}$  (32%). The weighted-average results are given in Table II, relative to a value of 100 for the ( $160 \rightarrow 158$ ) g.s. transition. Finally, Table III presents the summed cross-section ratios ( $\sum_{\theta, 5\text{--}70^\circ}$ ) relative to a value of 100 for each of the g.s. transitions in the  $^A\text{Gd}(p,t)^{A-2}\text{Gd}$  reactions. A comparison of the relative summed cross sections given in Table III and the  $23^\circ$  data in Ref. 6 shows qualitative agreement, especially when the  $2^+$  data are renormalized.

### III. NUCLEAR STRUCTURE AND DISCUSSION OF RESULTS

#### A. $0^+$ Transitions

The  $0^+$  states populated in these 18-MeV  $(p,t)$  reactions on the even Gd nuclei have previously been reported.<sup>5</sup> In all the stably deformed nuclei ( $^{158}\text{Gd}$ ,  $^{156}\text{Gd}$ ,  $^{154}\text{Gd}$ ) a single excited  $0^+$  state is observed with about  $\sim 15\%$  of the g.s. strength, although there are fluctuations of as much as a factor of 2. These fluctuations are apparent in the data of Tables I and III. In  $^{156}\text{Gd}$ , a second  $0^+$  state at 1168 keV<sup>14</sup> is observed (Figs. 2, 7) which has  $\sim 2.4\%$  of the g.s. strength (Table III). The present  $0^+$  data in Gd are very consistent with similar two-neutron transfer data previously reported on neighboring nuclei<sup>3,4,7,9</sup> (see also Ref. 6). However, the excited state  $0^+$  strength in this mass region ( $86 \leq N \leq 96$ ) is not nearly as stable as that found over a wider range of neutron numbers in the actinide region.<sup>13</sup>

Several theoretical attempts have been made to explain the relatively strong population of the  $0^+$  states seen in the  $(p,t)$  reaction. Van Rij and Kahana<sup>15</sup> and Bes, Broglia, and Nilsson<sup>16</sup> have considered a splitting of the pairing strength due to differences between equatorial and polar Nilsson orbits. Such calculations appear to give good agreement with the observed two-neutron transfer strength in the actinides.<sup>13,17</sup> Similar calculations, including also spin-quadrupole forces<sup>18</sup> have been considered by Abdulvagabova, Ivanova and Pyatov.<sup>19</sup> Belyaev and Rumiantsev<sup>20</sup> have suggested that the observed  $0^+$  strengths are due to the two-body spin-orbit force preventing mixing with other  $0^+$  degrees of freedom in the region of the Fermi surface. While these various models may all have enjoyed some degree of success in certain

TABLE I. Experimental results for 18-MeV (p, t) reactions on the even Gd nuclei.

$^{160}\text{Gd}(p, t)^{158}\text{Gd}$		$^{158}\text{Gd}(p, t)^{156}\text{Gd}$		$^{156}\text{Gd}(p, t)^{154}\text{Gd}$		$^{154}\text{Gd}(p, t)^{152}\text{Gd}$		$^{152}\text{Gd}(p, t)^{150}\text{Gd}$	
Exc <sup>a</sup> (keV)	$I^{\pi}, K$	Exc (keV)	$I^{\pi}, K$	Exc (keV)	$I^{\pi}, K$	Exc (keV)	$I^{\pi}, K$	Exc (keV)	$I^{\pi}, K$
$d\sigma(\theta)$ <sup>b</sup>	$\sum_e d\sigma^c$	$d\sigma(\theta)$ <sup>b</sup>	$\sum_e d\sigma^c$	$d\sigma(\theta)$ <sup>b</sup>	$\sum_e d\sigma^c$	$d\sigma(\theta)$ <sup>b</sup>	$\sum_e d\sigma^c$	$d\sigma(\theta)$ <sup>b</sup>	$\sum_e d\sigma^c$
( $\mu\text{b}/\text{sr}$ )	( $\mu\text{b}/\text{sr}$ )	( $\mu\text{b}/\text{sr}$ )	( $\mu\text{b}/\text{sr}$ )	( $\mu\text{b}/\text{sr}$ )	( $\mu\text{b}/\text{sr}$ )	( $\mu\text{b}/\text{sr}$ )	( $\mu\text{b}/\text{sr}$ )	( $\mu\text{b}/\text{sr}$ )	( $\mu\text{b}/\text{sr}$ )
0	0 <sup>+</sup> , 0	0	0 <sup>+</sup> , 0	0	0 <sup>+</sup> , 0	0	0 <sup>+</sup>	0	0 <sup>+</sup>
80	2 <sup>+</sup> , 0	89	2 <sup>+</sup> , 0	123	2 <sup>+</sup> , 0	344	2 <sup>+</sup>	638	2 <sup>+</sup>
261	4 <sup>+</sup> , 0	288	4 <sup>+</sup> , 0	371	4 <sup>+</sup> , 0	615	0 <sup>+</sup>	1135	3 <sup>-</sup>
539	6 <sup>+</sup> , 0	585	6 <sup>+</sup> , 0	681	0 <sup>+</sup> , 0	755	4 <sup>+</sup>	1209	0 <sup>+</sup>
977	1 <sup>-</sup> , 1	1049	0 <sup>+</sup> , 0	718	6 <sup>+</sup> , 0	931	2 <sup>+</sup>	1288	4 <sup>+</sup>
1042	3 <sup>-</sup> , 1	1129	2 <sup>+</sup> , 0	816	2 <sup>+</sup> , 0	1048	0 <sup>+</sup>	1430	2 <sup>+</sup>
1187	2 <sup>+</sup> , 2	1154	2 <sup>+</sup> , 2	996	2 <sup>+</sup> , 2	1110	2 <sup>+</sup>	1701	...
1196	0 <sup>+</sup> , 0	1168	0 <sup>+</sup> , 0	1048	4 <sup>+</sup> , 0	1121	3 <sup>-</sup>	1947	...
1260	2 <sup>+</sup> , 0	1243	1 <sup>-</sup> (0)	1190	...	1227	6 <sup>+</sup>	(1980)	0 <sup>+</sup>
1263	1 <sup>-</sup> , 0	1276	3 <sup>-</sup> (0)	1241	1 <sup>-</sup> , 0	1282	4 <sup>+</sup>	...	...
1265	3 <sup>+</sup> , 2	1298	4 <sup>+</sup> , 0	1253	3 <sup>-</sup> , 0	1315	1 <sup>-</sup>	...	...
1358	4 <sup>+</sup> , 2	1355	4 <sup>+</sup> , 2	1264	4 <sup>+</sup> , 2	1601	(2 <sup>+</sup> )	...	...
1452	0 <sup>+</sup> , 0	1408	5 <sup>-</sup>	1293	(0 <sup>+</sup> , 0)	1668	6 <sup>+</sup>	...	...
1517	2 <sup>+</sup> , 0	(1740)	0 <sup>+</sup>	1418	2 <sup>+</sup> , 0	...	...	...	...
1668	4 <sup>+</sup> , 0	...	...	1509	1 <sup>-</sup> , 1	...	...	...	...
...	...	...	...	1531	2 <sup>+</sup> , 2	...	...	...	...
...	...	...	...	1617	3 <sup>-</sup> , 1	...	...	...	...

<sup>a</sup> Excitation energies (keV) and spin assignments are taken from Refs. 14 and 28-33, except for the 0<sup>+</sup> states at 1048 and 1209 keV in  $^{152}\text{Gd}$  and  $^{150}\text{Gd}$ , respectively.

<sup>b</sup>  $d\sigma(\theta)$  is the differential cross section in  $\mu\text{b}/\text{sr}$  at (or near) the peak angle  $\theta$ . (5° for the 2<sup>+</sup> transitions and 30° for all other transitions.) The relative errors within each target nucleus are about ±7% for the strong transitions (>10  $\mu\text{b}/\text{sr}$ ) and 25% for the weak transitions.

<sup>c</sup> The linear sum of the differential cross sections (in  $\mu\text{b}/\text{sr}$ ) from 5.0 to 70.0° (lab) in 5.0° steps. The smooth curves shown in Figs. 6-11 were used to define the shapes of the angular distributions. See discussion in the text.

<sup>d</sup> All  $d\sigma(\theta)$  given at 30° (lab).

<sup>e</sup> Extrapolated values based on the smooth curves discussed in the text. Accurate only to ±20%.

<sup>f</sup> Only observed at 30°. Accurate to ±25%.

mass regions, it remain to be seen if they all, or in part, will be able to account for the observed  $0^+$  ( $p, t$ ) strengths over a wider range of mass and/or deformation. Certainly there is now available a sufficient collection of data with which to provide an adequate test.

The calculations of Ascutto and Sørensen,<sup>21</sup> in fact, have taken a further step towards this goal and provide the best over-all agreement to date with the available ( $p, t$ ) data in deformed nuclei. The force is conventional, pairing plus quadrupole; no new degrees of freedom are introduced. Their calculations are done in coupled channels (CC); the inclusion of multistep processes was found to be essential in reproducing both the shape and the detailed ratios of observed ( $p, t$ ) cross sections to  $K=0$  states. Indeed, their CC fits to the  $^{160}\text{Gd}(p, t)^{158}\text{Gd}$  data discussed herein, as well as to similar ( $p, t$ ) data on the Yb and W nuclei, are in good agreement with the experimental results.<sup>10, 21</sup> Their calculated cross section to the 1452-keV  $0^+$  ( $\beta$  vibration) in  $^{158}\text{Gd}$  agrees with the present data

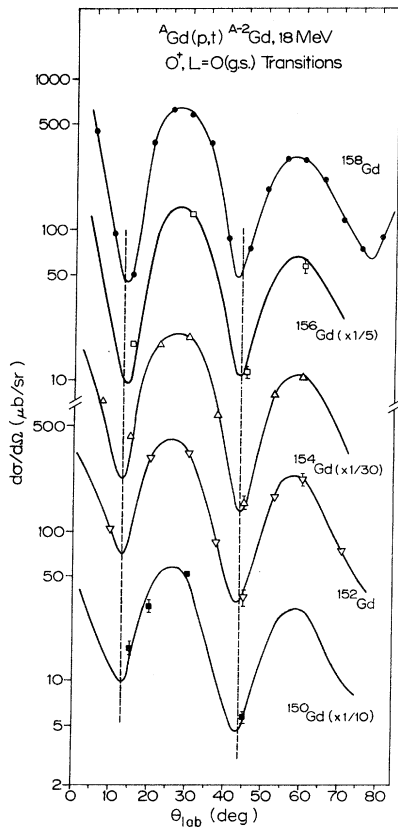


FIG. 6. The experimental ( $L=0$ ) angular distributions of the  $0^+$  ground states. Note the scale factors on some of the cross sections. The curves shown are discussed in the text; they have no theoretical significance and are drawn only to guide the eye. The vertical lines correspond to the position of diffraction minima.

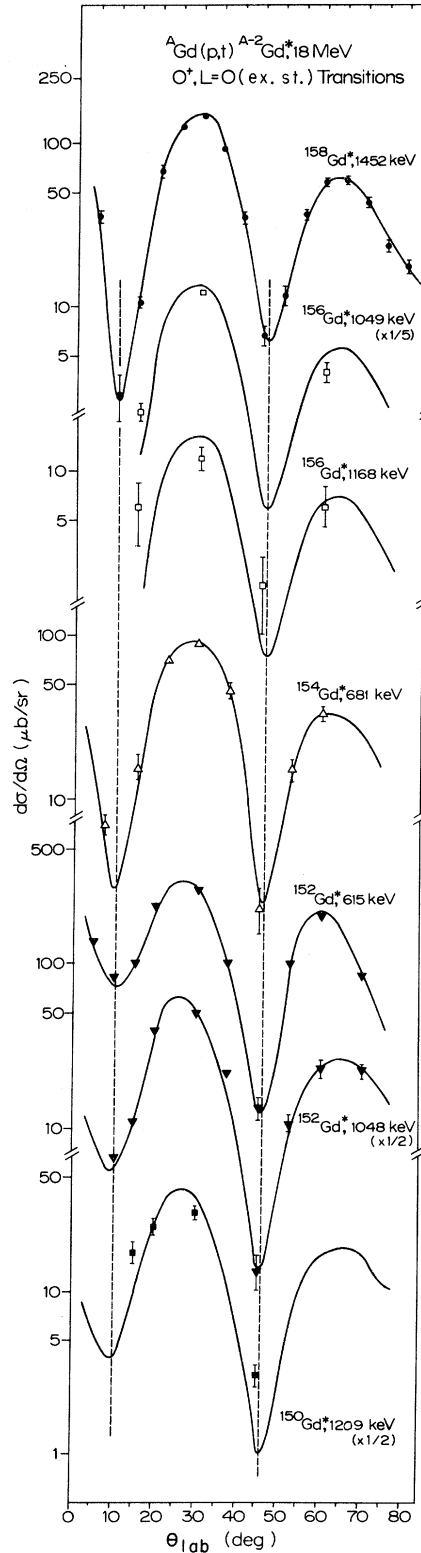


FIG. 7. The experimental ( $L=0$ ) angular distributions of the  $0^+$  excited states in the even Gd nuclei. See caption to Fig. 6.

to better than 20%. The agreement for the  $2^+$  states, discussed below, is of the same order.

In addition to the stably deformed nuclei discussed above, the present study provides information on the population of excited  $0^+$  states in  $^{152}\text{Gd}$  and  $^{150}\text{Gd}$ . The  $^{154}\text{Gd}(p, t)^{152}\text{Gd}$  reaction crosses the region of nuclear deformation at  $N=88$ . As previously observed in the Sm nuclei<sup>3,4,7</sup> and noted in Ref. 5, this sudden change in deformation is manifest in a sudden decrease in the  $(p, t)$  g.s. cross sections as well as in the appearance of two strongly populated excited  $0^+$  states. These effects are apparent in the data presented in Tables I–III, and have already been discussed in Ref. 5. See also Ref. 6.

Experimental  $L=0$  angular distributions for the  $0^+$   $(p, t)$  transitions on the even Gd nuclei are presented in Figs. 6 and 7. Figure 6 gives the g.s. transitions on all targets. The smooth curves

drawn are just to guide the eye; distorted-wave Born-approximation (DWBA) fits to the data are presented below. In the 158–156 and 152–150 reactions, data were obtained at only four angles and the curves shown in Fig. 6 are identical with those used to define the  $L=0$  angular distribution shape in neighboring nuclei (160–158 and 154–152, respectively). Such curves, of course, are not meant to be rigorously correct, but do serve as useful guidelines for a discussion of both the angular distribution shapes and integrated cross sections. They show, for example, the degree of stability of the  $L=0$  shapes over a  $Q$ -value range of 2 MeV, a feature which is common both in spherical<sup>22–24</sup> and in deformed nuclei<sup>7–9,13</sup> and often over very wide ranges of  $Q$  value.<sup>24</sup> The position of the minima in Fig. 6 are of interest. These are shown by the vertical lines drawn at a constant angle of 13 and 44° (lab) for the first and second minima, respectively.

Similar curves for the excited state  $0^+$  transitions are shown in Fig. 7. The over-all shapes of these transitions are very similar to the g.s. tran-

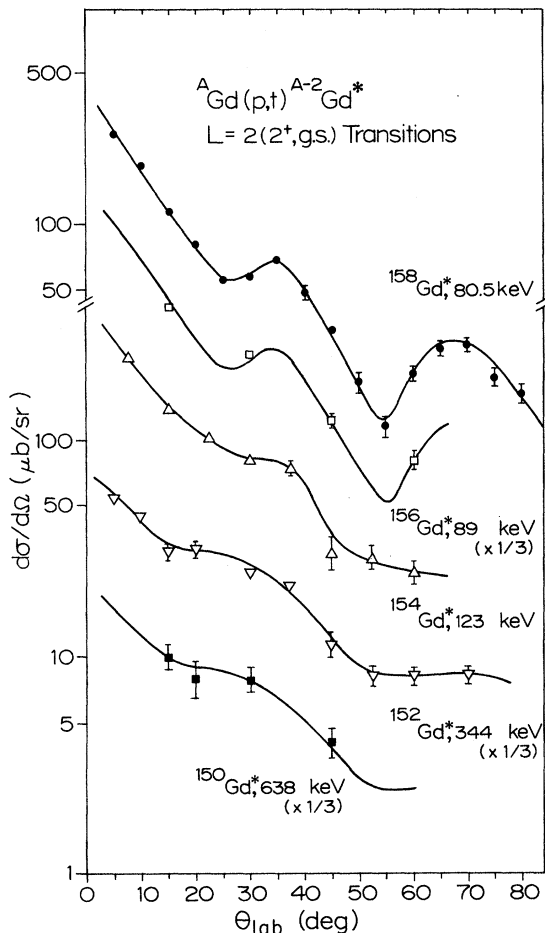


FIG. 8. The experimental ( $L=2, K=0$ ) angular distributions of the lowest-lying  $2^+$  states. Note the scale factors on some of the cross sections. The curves shown are discussed in the text; they have no theoretical significance and are drawn only to guide the eye.

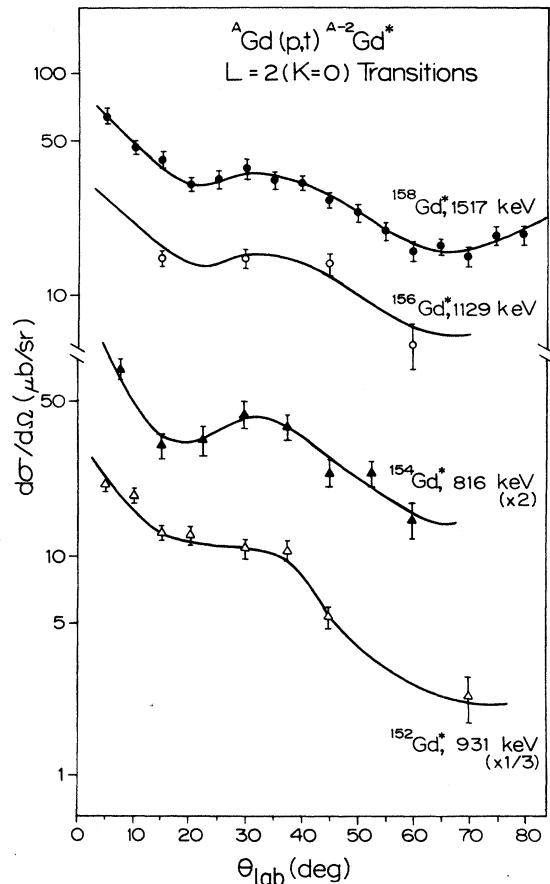


FIG. 9. The experimental ( $L=2, K=0$ ) angular distributions of the  $2^+$  ( $\beta$ -vibrational band) states in the even Gd nuclei. See caption to Fig. 8.

sitions of Fig. 6, but the minima appear to be systematically shifted; the first minimum is shifted in with respect to the g.s. minimum by  $\sim 3^\circ$  while the second minimum is shifted out by the same amount. If real, this shift cannot be a  $Q$ -value effect, since the g.s. transitions cover the same  $Q$ -value range; it thus suggests a nuclear structure and/or reaction mechanism effect. Similar effects have previously been reported in other deformed nuclei.<sup>9,13</sup> There is a tendency apparent in Figs. 6 and 7 for the depth of the  $\sim 10^\circ$  minimum to get shallower with decreasing  $Q$  value, which has been observed in other mass regions as well.<sup>22</sup>

### B. $2^+$ Transitions

In the present  $(p, t)$  study of the Gd nuclei, we are able to distinguish three distinct families of  $2^+$  transitions, based on the shapes of their angular distributions: the  $2^+$  member of the g.s. rotational band, the  $2^+$  member of the  $\beta$  vibration and the  $2^+$  ( $K=2$ )  $\gamma$  vibration. Similar conclusions have been reported in Ref. 6. In comparisons of

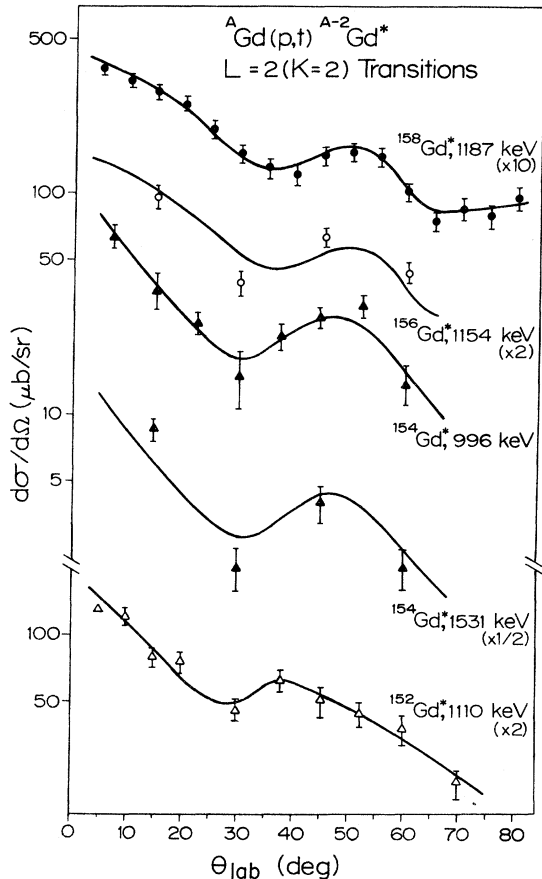


FIG. 10. The experimental ( $L=2, K=2$ ) angular distributions of the  $2^+$  ( $\gamma$ -vibrational) states in the even Gd nuclei. See caption to Fig. 8.

the present  $2^+$  ( $p, t$ ) data with those on neighboring nuclei, several interesting features emerge.

With reference to the data in Table I and III, we note that the summed cross section to the  $2^+$  member of the g.s. rotational band in each of the stably deformed Gd nuclei ( $^{158}\text{Gd}$ ,  $^{156}\text{Gd}$ ,  $^{154}\text{Gd}$ ) is essentially constant to within an experimental error of about 15% and, in addition, each is about 30% of the g.s. strength (the peak angle ratios of Table I are, in fact, closer to 50% of the g.s. strength). These data are consistent with the two-

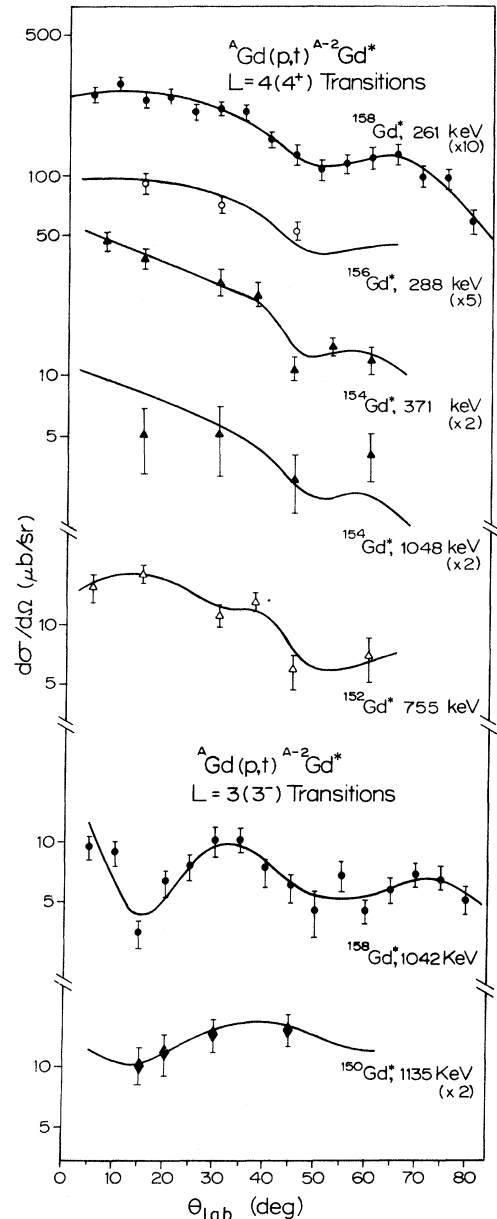


FIG. 11. The experimental angular distributions of the observed  $4^+$  and  $3^-$  states in the even Gd nuclei. See caption to Fig. 8.

neutron-transfer cross sections to similar  $2^+$  states in other deformed nuclei in this mass region<sup>3,4,6-9</sup> as well as in the tungsten and actinide regions.<sup>10,13,17</sup> This rotational  $2^+$  state is built on the pairing-favored ground state and thus it is not surprising that it should be relatively strongly populated in the (*p*, *t*) reaction.

In the DWBA calculations of Ref. 25 it was found necessary to introduce large  $\Delta N = 2$  mixtures into the normal Nilsson states, in order to account for the observed g.s.  $2^+$  cross sections. The need for such admixtures appears to be indicated by the one-neutron transfer data.<sup>26</sup> However, CC calculations were not performed in these calculations and inelastic processes may well play a decisive role.<sup>27</sup> Indeed, in the CC (*p*, *t*) calculations of Ascutto and Sørensen,<sup>21</sup> the (*p*, *t*) cross sections to the  $2^+$  members of both the g.s. and the  $\beta$ -vibrational bands in a variety of deformed nuclei are well reproduced.

As one moves from the rotational Gd nuclei to "quasirotational"  $^{152}\text{Gd}$  ( $N = 88$ )<sup>28,29</sup> and on to spherical  $^{150}\text{Gd}$  ( $N = 86$ ), the cross section to the lowest-lying  $2^+$  state changes markedly. In the  $^{154}\text{Gd}(p, t)^{152}\text{Gd}$  reaction, the  $2^+$  cross section to the 344-keV transition decreases, relative to the stably deformed nuclei, by essentially the same ratio as the g.s. transition. This result is evident in Ref. 6 also. The  $2^+$  transition then appears to be just as sensitive to the change in deformation at  $N = 88$  as the g.s. transition discussed earlier. The same effect on the (g.s.)  $2^+$  cross section at  $N = 88$  has previously been noted in the  $^{150}\text{Sm}(t, p)^{152}\text{Sm}$  reaction<sup>7</sup> and also in the inverse (*p*, *t*) reaction,<sup>4</sup> although there appear to be some differences in the (*p*, *t*) data.<sup>3,4</sup> In the  $^{152}\text{Gd}(p, t)^{150}\text{Gd}$  reaction, the cross section to the 638-keV  $2^+$  state changes sharply; the summed cross section is down relative to those discussed above by roughly a factor of 4. Part of this decrease will be due to kinematic effects; DWBA calculations, however, pre-

TABLE II. The relative g.s. cross section for 18-MeV (*p*, *t*) reactions on the Gd nuclei.

Reaction	Relative cross section <sup>a</sup>
160→158	100±7
158→156	108±8
156→154	98±7
154→152	48±6
152→150	94±9
157→155	63±6

<sup>a</sup> These cross sections are a weighted average of several runs, as discussed in the text, and were obtained at 30° (lab).

dict a change of only 30%. No other  $2^+$  strength was observed in  $^{150}\text{Gd}$ . This result in itself, namely, that the 152→150 (*p*, *t*) reaction between two predominantly spherical nuclei in Gd weakly populates only a single  $2^+$  state (Tables I and III), is contrary to both the (*t*, *p*) and (*p*, *t*) results in Sm,<sup>4,7</sup> where more than a single  $2^+$  level is observed with total cross sections comparable in strength with the rotational  $2^+$  cross sections.

The  $K=0$  ( $\beta$ ) and  $K=2$  ( $\gamma$ )  $2^+$  (*p*, *t*) transitions in the even Gd nuclei (158→152) are, on the average, about 30% as strong as the first  $2^+$  state and therefore about 10% of the g.s. strength (Table III). These results are also consistent with similar data in other nuclei.<sup>3,4,7-10,13</sup> The assignments of  $K=0$  and  $K=2$  have all been made previously.<sup>14,28,30-32</sup> From the data in Table I and III it can easily be seen that there is no correlation in the cross section with  $K=0$  or  $K=2$  in the (*p*, *t*) reaction on Gd. For example, in the 160→158 reaction, the  $2^+$ ,  $K=0$  transition is roughly twice the strength of the  $2^+$ ,  $K=2$  transition, whereas, in the 158→156 and 156→154 reactions, the reverse is true. These results are somewhat different from those found in the Dy and Er nuclei,<sup>9</sup> where the  $2^+$   $\gamma$  vibrations appear to be preferentially populated. In the transitional nucleus  $^{152}\text{Gd}$ ,

TABLE III. Relative summed cross sections for 18-MeV (*p*, *t*) reactions on the even Gd nuclei.

$I^\pi, K$	160→158		158→156		156→154		154→152		152→150	
	Exc (keV)	$\sum_R^a$	Exc (keV)	$\sum_R$	Exc (keV)	$\sum_R$	Exc (keV)	$\sum_R$	Exc (keV)	$\sum_R$
$0^+, 0$	0	100	0	100	0	100	0	100	0	100
$2^+, 0$	80	26.7	89	29.0	123	37.9	344	38.1	638	8.7
$4^+, 0$	261	6.6	288	4.3	371	4.6	755	5.6	1288	~0.5
$0^+, 0$	1452	19.3	1049	7.9	681	13.2	615	76.1	1209	12.4
$2^+, 0$	1517	11.2	1129	4.5	816	5.4	931	16.0	...	...
$2^+, 2$	1187	6.6	1154	11.4	996	9.9	1110	16.2	...	...
$0^+, 0$	1196	<0.2	1168	2.4	1293	<0.2	1048	28.0	...	...
$3^-$	1042	2.4	1276	~1.5	1251	<0.2	1123	~0.5	1135	2.7

<sup>a</sup>  $\sum_R$  is the summed cross section of Table I [ $\sum_{\theta} (d\sigma)$ , 5–70°] relative to a value of 100 for each Gd (*p*, *t*) g.s. transition.



the  $2^+$  states observed in the 154–152 reaction are populated with equal intensity. From the ( $d, d'$ ) results<sup>33</sup> these two states are also known to have comparable  $B(E2)$  values. The same result has been observed in the  $^{152}\text{Sm}(p, t)^{150}\text{Sm}$  reaction.<sup>4</sup> The only other known  $2^+$  state excited with a measurable intensity (4% of g.s.) in this experiment is the one at 1531 keV in the 156–154 reaction, which is believed to be a  $K=2$  state.<sup>32</sup> The angular distribution shapes presented below are indeed in agreement with a  $K=2$  assignment. A level at 1601 keV in  $^{152}\text{Gd}$  has been suggested as a  $2^+$  state,<sup>28</sup> but an angular distribution was not obtainable. The relatively strong peak at  $30^\circ$  in this experiment, if anything, suggests a  $0^+$  assignment.

While the distinction between  $K=2$  and  $K=0$  cannot be made on the basis of ( $p, t$ ) cross sections to the  $2^+$  states, indications are that such a distinction can be made on the basis of the shapes of the angular distributions in the Gd nuclei. The  $2^+$  angular distributions are shown in Figs. 8–10; Fig. 8 presents the  $2^+$  (g.s.,  $K=0$ ) transitions, Fig. 9 the  $2^+_{\beta}$  ( $K=0$ ), and Fig. 10 the  $2^+_{\gamma}$  ( $K=2$ ) angular distributions. As in the  $L=0$  transitions discussed above, curves have been drawn through the data points as a guide to the eye—the more complete data in the 160–158 and 154–152 reactions have again been used to define the curves for the neighboring 158–156 and 152–150 reactions, respectively. The  $2^+$  (g.s.) angular distribution shapes shown in Fig. 8 have a highly reproducible structure and, as discussed below, are very poorly accounted for by DWBA calculations. Similar results have been found elsewhere.<sup>3, 4, 6–10, 13</sup>

As can be seen from Figs. 9 and 10 there is a definite distinction in shape between the  $2^+_{\beta}$  and  $2^+_{\gamma}$  transitions, which is evident in both the region of  $30^\circ$  and  $50^\circ$ . Note that the transitions labeled  $K=0$  in Fig. 9 generally show a peaking around  $30^\circ$  but a falloff in cross section in the region of  $50^\circ$ , while the transitions labeled  $K=2$  in Fig. 10 tend to show the opposite effect. The effect is sufficiently reproducible to be believed and as such appears to be unique to the ( $p, t$ ) reaction in Gd. Similar conclusions have been reached in Ref. 6. Indeed, on the basis of both previous data in other nuclei and current CC calculations, it has generally been accepted that little stability can be expected for  $L=2$  angular distribution shapes in the ( $p, t$ ) reaction on deformed nuclei.<sup>3, 4, 7–10, 13, 21, 34–36</sup> This expectation is, in fact, contrary to the generally stable shapes observed in ( $p, t$ ) reactions to  $2^+$  levels in spherical nuclei.<sup>22–24, 37</sup> We note that the angular distribution shapes seen in the 154–152  $2^+$  transitions are somewhat at variance with the above pattern, which is perhaps not surprising in view of the “transitional” nature of  $^{152}\text{Gd}$ .

### C. $4^+$ Transitions

The ( $p, t$ )  $4^+$  transitions in the deformed Gd nuclei are generally weak; in essence, only the  $4^+$  member of the g.s. rotational band is seen with any intensity, about 5% of the g.s. cross section (Tables I and III). These data are again quite consistent with similar data in this mass region. The gradual decrease apparent in the  $4^+$  cross sections with decreasing  $A$  is consistent with DWBA calculations of the kinematics. However, there may also be some effect in the 154–152 reaction due to the  $N=88$  crossing, as there is for the  $0^+$  and  $2^+$  transitions discussed above. The  $4^+$  transitions leading to the 1288-keV level in spherical  $^{150}\text{Gd}$  is much weaker than the  $4^+$  (g.s.) transitions in the deformed Gd nuclei.

The experimental  $4^+$  angular distribution shapes are presented in Fig. 11. As with the  $0^+$  and  $2^+$  transitions, there is also a similarity in shape in these  $4^+$  angular distributions although in some cases the error bars on the data points are large. There is more fluctuation in shape apparent in the  $4^+$  ( $p, t$ ) transitions reported in the Dy and Er data of Ref. 9, and in the Sm( $p, t$ ) data of Ref. 4, as there is also in the  $2^+$  transitions. There was also measurable (but small) ( $p, t$ ) yield observed to higher-lying  $4^+$  states in the deformed Gd nuclei. An example is the 1048-keV ( $4^+$ ,  $K=0$ ) transition in the 156–154 reaction. The angular distribution is shown, albeit with large error bars, in Fig. 11. The summed cross section for this transition (Table I) is only 1% of the g.s. cross section. The 1668-keV ( $4^+$ ,  $K=0$ ) transition in the 160–158 reaction has a similar yield. In the theoretical calculations of Ascuitto and Sørensen,<sup>21</sup> the  $4^+$  member of the g.s. rotational band in the  $^{160}\text{Gd}(p, t)^{158}\text{Gd}$  reaction is accounted for equally well in both their CC and DWBA calculations but there is a sizable difference in the transition strengths predicted to the  $4^+$  member of the  $K=0$  ( $\beta$ -vibrational) band. In fact, their CC calculations again give the best agreement with the observed strength (Table I) to the 1668-keV transition in  $^{158}\text{Gd}$ .

### D. Other Transitions

The only  $6^+$  states observed in this experiment were the  $6^+$  members of the g.s. rotational bands. Angular distributions were not obtainable. The maximum  $6^+$  cross section seen (at  $30^\circ$ ) was to the 718-keV state in the 156–154 reaction, about 1% of the g.s. cross section. Unlike the  $4^+$  transitions, no higher-lying  $6^+$  states were observed in these experiments.

The known  $1^-$  states in the Gd nuclei were essentially not populated ( $\approx 0.3\%$  of the g.s. cross section). On the other hand, there was measurable

strength in some cases for  $3^-$  transitions, comparable with that of the  $6^+$  transitions. Angular distributions were obtained for  $3^-$  transfers in the  $160 \rightarrow 158$  and  $152 \rightarrow 150$  reactions; these are shown in Fig. 11 along with the  $4^+$  transfers previously discussed. In both these cases the  $3^-$  cross sections were  $\geq 2\%$  of the g.s. strengths (Table III). We note that the  $3^-$  states at 1253 and 1121 keV in  $^{154}\text{Gd}$  and  $^{152}\text{Gd}$ , respectively,<sup>33</sup> are not seen with any measurable strength. There are  $3^-$  states seen in the Sm nuclei,<sup>4,7</sup> but in the Dy and Er nuclei, no  $1^-$  or  $3^-$  states are populated in the ( $p, t$ ) reaction.<sup>9</sup>

In the  $^{158}\text{Gd}(p, t)^{156}\text{Gd}$  reaction, a  $5^-$  level at 1408 keV is populated as strongly as the  $3^-$  level; no  $5^-$  states were seen in any of the other Gd nuclei. In none of the Gd nuclei studied was there any population of known  $3^+$  and  $5^+$  states, which is at least consistent with the expected population of only natural parity states in the ( $p, t$ ) reaction.

#### IV. DISTORTED-WAVE CALCULATIONS

In the following, we present some theoretical angular distributions, calculated within the usual DWBA prescription, calculated within the usual DWBA prescription. No nuclear structure information is included. The optical-model parameters used in the DWBA analysis were taken directly from the  $DX$  combination of Ref. 22; no further variation of these parameters was attempted. In addition to the generally good fits to 20-MeV ( $p, t$ ) reactions on the even Sn nuclei,<sup>22</sup> this potential also represents a reasonably good "average fit" to the elastic scattering data in the  $A \approx 160$  mass region.<sup>38</sup> In fact, the  $DX$  potential of Ref. 22 is very similar to the ones used in Ref. 9 and in the theoretical calculations of Ref. 21. The  $AX$  combination of Ref. 22 and the triton potential of Ref. 39 were also tried in the DWBA calculations. Both choices gave rather poor agreement with the data, particularly the latter choice. However, it is probably not meaningful to examine optical-model "sensitivities" in any detail in this mass region, in view of the large inelastic (CC) contributions to the cross section.<sup>21</sup>

In the Gd nuclei, the Nilsson orbits in the region of the Fermi surface arise from both the  $N=5$  (e.g.,  $2f_{7/2}$ ) and  $N=6$  (e.g.,  $1i_{13/2}$ ) major oscillator shells. In Fig. 12 are shown representative DWBA fits to the  $0^+$  ( $L=0$ ) transitions assuming a pure  $(2f_{7/2})^2$  transfer. In the notation of Ref. 40,  $(2f_{7/2})^2$  corresponds predominantly to an  $L=0$ ,  $N=6$  center-of-mass motion of the transferred pair. Only the shapes are significant in the present calculations and each calculated curve in Fig. 12 is individually and arbitrarily normalized to the data. The DWBA curves shown were obtained

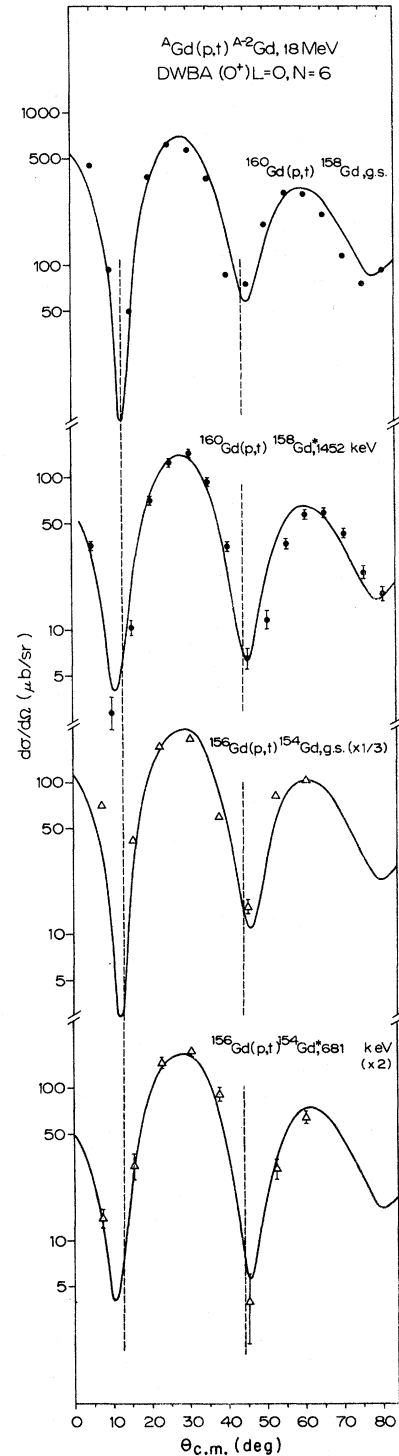


FIG. 12. DWBA calculated angular distributions of the  $0^+$  states populated in the  $^{160,156}\text{Gd}(p, t)^{158,154}\text{Gd}$  reactions. Note the scale factors on some of the transitions. The DWBA curves have been separately normalized to the data. The vertical dashed lines are the same as those shown in Figs. 6 and 7.

with a Woods-Saxon form factor using the Colorado code DWUCK which employs the Bayman-Kallio<sup>41</sup> method of constructing the two-nucleon form factor. Identical curves were obtained with a harmonic-oscillator (with matched hankel-function) form factor, as can be seen in Ref. 5. The overall quality of the DWBA fits to the  $0^+$  transitions is excellent, especially when considering the method by which the potential was chosen. This in itself suggests that the shapes of the  $0^+$  transitions are not much affected by the inclusion of inelastic processes in the transfer calculation, a conclusion which is supported by CC calculations in this mass region.<sup>21, 34-36</sup> The  $0^+$  transitions on deformed nuclei, in fact, are generally well fitted by DWBA calculations<sup>9, 13, 21, 34, 36</sup> This result is certainly not true of the  $2^+$  transitions discussed below.

The vertical lines shown at 13 and 44° in Fig. 12 are the experimental positions of the g.s. minima (cf. Figs. 6 and 7). We note that the  $\approx 3^\circ$  shifts previously referred to in the position of the minima in the  $0^+$  transitions are generally not reproduced by the DWBA calculations. However, these shifts are small, to be sure, and may be more of perspective than of physics. Similar shifts have been reported in Refs. 9 and 13. These authors have been able to obtain better DWBA fits to the excited state  $0^+$  transitions by employing single-particle orbits which lie above the Fermi surface. While such calculations may demonstrate the sensitivity of the calculated  $L=0$  shapes to changes in form factor, they hardly make any physical sense; if anything, the  $(p, t)$  transitions to excited states would be more sensitive to single-particle orbits below the Fermi surface. Indeed, no  $(t, p)$  strength has been found to excited  $0^+$  states in the actinides.<sup>17</sup> Such  $0^+$  "shifts" are just as likely to be due to interference effects in the accompanying inelastic processes. We have repeated the  $(p, t)$  calculations in Gd assuming both pure  $N=5$  and  $N=7$  for the center-of-mass motion of the transferred pair. (The shape is insensitive to smaller  $N$  components in all cases.) The best over-all fits for both the g.s. and the excited state  $0^+$  transitions were obtained with the predominantly  $N=6$  form factor; i.e., one corresponding to the transfer of a  $(2f_{7/2})^2$  pair of neutrons for both states.

In Fig. 13 are shown the DWBA fits for the  $2^+$ ,  $3^-$ , and  $4^+$   $(p, t)$  transitions found in the 18-MeV  $^{160}\text{Gd}(p, t)^{158}\text{Gd}$  reaction. As for the g.s. transitions, the form factors for the  $2^+$  and  $4^+$  transitions were constructed from a pure  $(2f_{7/2})^2$  transfer. The  $3^-$  configuration was assumed to be  $(2f_{7/2}, 2d_{3/2})$ . Each calculated curve is again arbitrarily normalized to the data.

By far the poorest DWBA fit obtained in this study is to the  $2^+$  member of the g.s. rotational

band. This result appears to be generally true for  $(p, t)$  reactions on deformed nuclei.<sup>9, 10, 13, 21, 33-36</sup> The inclusion of inelastic channels in the transfer process markedly improves the agreement with experiment for this state; such CC calculations<sup>21, 33-36</sup> appear to be vital to a proper understanding of the reaction mechanism, at least for these g.s.  $2^+$  states. On the other hand, angular distributions to the higher-lying  $2^+$  states in

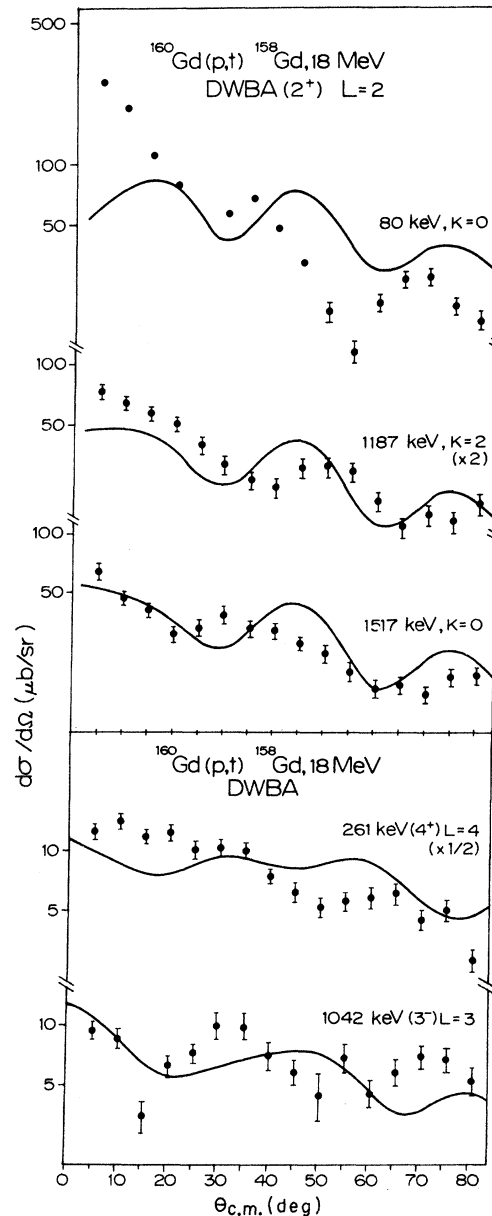


FIG. 13. DWBA calculated angular distributions to the  $2^+$ ,  $3^-$ , and  $4^+$  states observed in the  $^{160}\text{Gd}(p, t)^{158}\text{Gd}$  reaction. Note the scale factors on some of the transitions. The DWBA curves have been separately normalized to the data.

$^{158}\text{Gd}$  (1187 keV,  $K=2$  and 1517 keV,  $K=0$ ) agree much better with the calculated DWBA curves, as can be seen in Fig. 13. The CC calculations of Ref. 21 for the  $^{160}\text{Gd}(p, t)^{158}\text{Gd}$  reaction do not yield any better fit to the 1517-keV level than the DWBA fit presented here, which is a clear difference with the  $2^+$  transition to the g.s. band. Certainly for this  $2^+$ ,  $K=0$  state at least, no distinction between DWBA and CC can be made on the basis of shape alone; indeed, the relative magnitudes in the calculations of Ref. 21 vary little also. The  $2^+$ ,  $K=2$  transition in  $^{158}\text{Gd}$  was not considered in those calculations.

The DWBA fits to the 261-keV  $4^+$  (g.s. band) and to the 1042-keV  $3^-$  states in the  $^{160}\text{Gd}(p, t)^{158}\text{Gd}$  reaction are also shown in Fig. 13. The envelopes of the calculated curves agree well with those of the data but clearly a detailed fit to the shape is lacking. On the other hand, the  $4^+$  CC calculation for  $^{158}\text{Gd}$  in Ref. 21 offers no significant improvement.

The DWBA fits to the ( $p, t$ ) reactions on the other deformed Gd nuclei were of the same quality as those seen here, and are thus not presented. The fits obtained in spherical  $^{150}\text{Gd}$  were not as good

as those given in Figs. 12 and 13, nor were they as good as those obtained on the spherical Sn nuclei,<sup>22</sup> from which the  $DX$  potential was obtained. However, it is difficult to make an assessment of this difference in view of the fact that there are relatively few data points in the present study of the 152–150 reaction.

Finally, we would like to mention that the  $^{157}\text{Gd}(p, t)^{155}\text{Gd}$  g.s. cross section between two odd-spin states ( $\frac{3}{2}^- | 521 |$ ), which was obtained from impurity peaks in several targets (Table II), is only 60% of the g.s. cross section obtained in the other deformed (even) targets. This reduction is not a DWBA (kinematic) effect and is most probably the result of the Pauli principle, which can be very effective in blocking certain orbits in the ( $p, t$ ) reaction, notably those of small angular momenta.<sup>42</sup>

#### ACKNOWLEDGMENTS

Two of us (D. G. Fleming and C. Günther) would like to thank Professor A. Bohr and the staff of the Niels Bohr Institute for their hospitality and support during the course of this work.

- 
- <sup>1</sup>J. B. Ball, R. L. Auble, J. Rapaport, and C. B. Fulmer, Phys. Lett. **30B**, 533 (1969); T. Udagawa, T. Tamura, and T. Izumoto, *ibid.* **35B**, 129 (1971); K. Yagi, K. Sato, Y. Aoki, T. Udagawa, and T. Tamura, Phys. Rev. Lett. **29**, 1334 (1972); J. D. Sherman, B. G. Harvey, D. L. Hendrie, M. S. Zisman, and B. Sørensen, Phys. Rev. C **6**, 1082 (1972); T. J. Mulligan, E. R. Flynn, O. Hansen, R. F. Casten, and R. K. Sheline, *ibid.* **6**, 1802 (1972).
- <sup>2</sup>S. Hinds, J. H. Bjerregaard, O. Hansen, and O. Nathan, Phys. Lett. **14**, 48 (1965); R. Chapman, W. McLatchie, and J. E. Kitching, Phys. Lett. **31B**, 292 (1970). See also R. F. Casten, E. R. Flynn, O. Hansen, T. Mulligan, R. K. Sheline, and P. Kienle, Phys. Lett. **32B**, 45 (1970).
- <sup>3</sup>W. McLatchie, J. E. Kitching, and W. Darcey, Phys. Lett. **30B**, 529 (1969); P. Debenham and N. M. Hintz, Phys. Rev. Lett. **25**, 44 (1970); W. McLatchie, W. Darcey, and J. E. Kitching, Nucl. Phys. **A159**, 615 (1970).
- <sup>4</sup>P. Debenham and N. M. Hintz, Phys. Rev. Lett. **25**, 44 (1970); Nucl. Phys. **A195**, 385 (1972).
- <sup>5</sup>D. G. Fleming, C. Günther, G. B. Hagemann, B. Herskind, and P. O. Tjøm. Phys. Rev. Lett. **27**, 1235 (1971).
- <sup>6</sup>Th. W. Elze, J. S. Boyno, and J. R. Huizenga, Nucl. Phys. **A187**, 473 (1972).
- <sup>7</sup>J. H. Bjerregaard, O. Hansen, O. Nathan, and S. Hinds, Nucl. Phys. **86**, 145 (1966).
- <sup>8</sup>M. Oothoudt, N. M. Hintz, and P. Vedelsby, Phys. Lett. **32B**, 270 (1970).
- <sup>9</sup>J. V. Maher, J. J. Kolata, and R. W. Miller, Phys. Rev. C **6**, 358 (1972).
- <sup>10</sup>C. H. King, R. J. Ascutto, N. Stein, and B. Sørensen, Phys. Rev. Lett. **29**, 71 (1972); See also, ANL Report No. PHY-1972H, March 1972 (unpublished).
- <sup>11</sup>R. W. Gales, R. A. Warner, W. C. McHarris, and W. H. Kelly, Phys. Rev. C **6**, 587 (1972); Phys. Rev. Lett. **29**, 802 (1972).
- <sup>12</sup>T. Kammuri and H. Yoshida, Nucl. Phys. **A117**, 27 (1968); E. Y. Berlowitch, Acta Phys. Pol. **A38**, 645 (1970); G. Holzwarth, Nucl. Phys. **A156**, 511 (1970); T. Takemasa, M. Sakagami, and M. Sano, Phys. Lett. **37**, 473 (1971).
- <sup>13</sup>J. V. Maher, J. R. Erskine, A. M. Friedman, J. P. Schiffer, and R. H. Siemssen, Phys. Rev. Lett. **25**, 302 (1970); J. R. Comfort, J. R. Duray, and W. J. Braithwaite, Phys. Rev. C **4**, 277 (1971); J. V. Maher, J. R. Erskine, A. M. Friedman, R. H. Siemssen, and J. P. Schiffer, *ibid.* **5**, 1380 (1972).
- <sup>14</sup>A. Bäcklin, *International Symposium on Neutron Capture Gamma-Ray Spectroscopy, Studsvik, Sweden, August, 1969* (International Atomic Energy Agency, Vienna, Austria, 1969), p. 149; H. L. Nielsen, N. Rud, and K. Wilsky, Phys. Lett. **30B**, 169 (1969).
- <sup>15</sup>W. I. van Rij and S. H. Kahana, Phys. Rev. Lett. **28**, 50 (1972).
- <sup>16</sup>D. R. Bes, R. A. Broglia, and B. Nilsson, Phys. Lett. **40B**, 338 (1972).
- <sup>17</sup>R. F. Casten, E. R. Flynn, J. D. Garrett, O. Hansen, T. J. Mulligan, D. R. Bes, R. A. Broglia, and B. Nilsson, Phys. Lett. **40B**, 333 (1972).
- <sup>18</sup>N. I. Pyatov, Ark. Fys. **36**, 667 (1967); A. A. Kuliev, and N. I. Pyatov, Nucl. Phys. **A106**, 689 (1968).
- <sup>19</sup>S. K. Abdulvagabova, S. P. Ivanova, and N. I. Pyatov,

- Phys. Lett. 38B, 215 (1972).
- <sup>20</sup>S. T. Belyaev, *Yad. Fiz.* 4, 936 (1966) [transl.: *Sov. J. Nucl. Phys.* 4, 671 (1967)]; S. T. Belyaev and B. A. Rumiantsev, *Phys. Lett.* 30B, 444 (1969).
- <sup>21</sup>R. J. Ascutto and B. Sørensen, *Nucl. Phys.* A190, 297 309 (1972).
- <sup>22</sup>D. G. Fleming, M. Blann, H. W. Fulbright, and J. A. Robbins, *Nucl. Phys.* A157, 1 (1970).
- <sup>23</sup>J. H. Bjerregaard, O. Hansen, O. Nathan, L. Vistien, R. Chapman, and S. Hinds, *Nucl. Phys.* A110, 1 (1968); *ibid.* A131, 481 (1969); E. R. Flynn and J. G. Beery, *Phys. Rev. Lett.* 24, 143 (1970).
- <sup>24</sup>D. G. Fleming, J. Cerny, C. C. Maples, and N. K. Glendenning, *Phys. Rev.* 166, 1012 (1968).
- <sup>25</sup>R. A. Broglia, C. Riedel, and T. Udagawa, *Nucl. Phys.* A135, 561 (1969); T. Udagawa, *ibid.* A164, 484 (1971).
- <sup>26</sup>P. O. Tjømm and B. Elbek, *K. Dan. Vidensk. Selsk. Mat.-Fys. Medd.* 36, No. 8 (1967) and references contained therein; R. K. Sheline, M. J. Bennet, J. W. Dawson, and Y. Shida, *Phys. Lett.* 26B, 14 (1967); R. K. Sheline and Y. Shida, *ibid.* 26B, 210 (1967); I. Kanestrøm, P. O. Tjømm, and J. Bang, *Nucl. Phys.* A164, 664 (1971).
- <sup>27</sup>N. K. Glendenning, *Nucl. Phys.* A168, 575 (1970); R. J. Ascutto *et al.*, *Phys. Rev. Lett.* 29, 1106 (1972); H. Schulz, H. J. Wiebicke, and F. A. Gareev, *Nucl. Phys.* A180, 625 (1972).
- <sup>28</sup>K. Ya. Gromov, V. V. Kuznetsov, M. Y. Kuznetsova, M. Finger, J. Urbanec, O. B. Nielsen, K. Wilsky, O. Skilbreid, and M. Jørgensen, *Nucl. Phys.* A180, 625 (1972); E. Ya. Luve, L. K. Peker, and P. T. Prokof'ev, *Izv. Akad. Nauk SSSR Ser. Fiz.* 32, 74 (1968) [transl.: *Bull. Acad. Sci. USSR* 32, 74 (1968)]; L. Varnell, J. D. Bowman, and J. Trischuk, *Nucl. Phys.* A127, 270 (1969).
- <sup>29</sup>M. Sakai, *Nucl. Phys.* A104, 301 (1967); Y. Gono, *International Symposium on Nuclear Structure, Dubna, 1968* (International Atomic Energy Agency, Vienna, Austria, 1969); L. L. Riedinger, N. R. Johnson, and J. H. Hamilton, *Phys. Rev. C* 2, 2358 (1970); W. W. Bowman, T. T. Sugihara, and F. R. Hamiter, *ibid.* 3, 1275 (1971).
- <sup>30</sup>C. J. Paperiello, E. G. Funk, and J. W. Mihelich, *Nucl. Phys.* A140, 261 (1970); H. Bader, M.Sc. thesis, University of Muenchen, 1970 (unpublished).
- <sup>31</sup>M. Fujioka, *Nucl. Phys.* A153, 337 (1970); D. J. McMillan, J. H. Hamilton, and J. J. Pinajian, *Phys. Rev. C* 4, 542 (1971); J. H. Hamilton, M. Fujioka, J. J. Pinajian, and D. J. McMillan, *ibid.* 5, 1800 (1972).
- <sup>32</sup>L. C. Whitlock, J. H. Hamilton, and A. V. Ramayya, *Phys. Rev. C* 3, 313 (1971); L. L. Riedinger, D. C. Sousa, E. G. Funk, and J. W. Mihelich, *ibid.* 4, 1352 (1971); S. M. Ferguson, R. Heffner, and H. Ejiri, *Phys. Lett.* 35B, 214 (1971).
- <sup>33</sup>R. Bloch, B. Elbek, and P. O. Tjømm, *Nucl. Phys.* A91, 576 (1967).
- <sup>34</sup>R. J. Ascutto, N. K. Glendenning, and B. Sørensen, *Phys. Lett.* 34B, 17 (1971).
- <sup>35</sup>T. Tamura, D. R. Bes, R. A. Broglia, and S. Landowne, *Phys. Rev. Lett.* 26, 158 (1971); 25, 1507 (1970).
- <sup>36</sup>T. Udagawa, T. Tamura, and T. Izumoto, *Phys. Lett.* 35B, 129 (1971).
- <sup>37</sup>N. K. Glendenning, *Phys. Rev.* 156, 1344 (1967); S. M. Smith, C. Moazed, A. M. Bernstein, and P. G. Roos, *ibid.* 169, 951 (1968).
- <sup>38</sup>F. D. Becchetti and G. W. Greenlees, *Phys. Rev.* 182, 1190 (1969); E. R. Flynn, D. D. Armstrong, J. G. Beery, and A. G. Blair, *ibid.* 182, 1113 (1969).
- <sup>39</sup>M. Jaskola, K. Nybø, P. O. Tjømm, and B. Elbek, *Nucl. Phys.* A96, 52 (1967).
- <sup>40</sup>N. K. Glendenning, *Phys. Rev.* 137, B102 (1965); I. S. Towner and J. C. Hardy, *Adv. Phys.* 18, 401 (1969).
- <sup>41</sup>B. F. Bayman and A. Kallio, *Phys. Rev.* 156, 1121 (1967).
- <sup>42</sup>D. G. Fleming, M. Blann, and H. W. Fulbright, *Nucl. Phys.* A163, 410 (1971).